Frequency conversion in aperiodic quasi-phase-matched structures

G. Kh. Kitaeva
Faculty of Physics, M.V. Lomonosov Moscow State University, 119991 Moscow, Russia
(Received 15 June 2007; published 26 October 2007)

The influence of disordering of one-dimensional quasi-phase-matched structures in nonlinear-optical crystals on the spectral characteristics of parametric processes is studied in the general form, taking into consideration arbitrary spatial distribution of the second-order susceptibility, sum- and difference-frequency interactions in the forward and backward directions, and continuous-wave and pulsed pumping. It is shown that, at the initial low-gain stages of all processes, the impact of the medium spatial structure can be described in terms of a single functional parameter, nonlinear transfer function (*T-function*). Expressed in terms of dimensionless phase mismatches, the *T-function* is considered as a universal characteristic of the structured medium. The method of its direct measurement is proposed, based on spontaneous parametric down-conversion. Examples of the *T-function* approach are demonstrated for short-pulse second harmonic generation, as well as for generation and detection of spectral-shaped terahertz signals.

DOI: 10.1103/PhysRevA.76.043841 PACS number(s): 42.65.Ky, 78.40.Pg, 78.67.−n, 42.79.Nv

I. INTRODUCTION

Advantages of periodically structured nonlinear-optical media have been known since the 1960s [1,2] and, starting from the 1980 [3–5], are widely used for quasiphase matching (QPM) in various nonlinear frequency conversion processes [6]. Now the concept of QPM enables one to provide an effective energy exchange between almost any two monochromatic waves from different spectral ranges, from terahertz [7–10] up to ultraviolet [11,12] ranges. QPM structures can be sorted according to whether it is the linear [13,14] or nonlinear [1–12,15] optical inhomogeneity that is crucial for their operation. At present, most efficient for applications are structures of the second type—periodically poled crystals with regular domain gratings, such as lithium niobate, lithium tantalate, KTP, and others, in which the sign of the second-order susceptibility periodically changes at ferroelectric domain boundaries while the linear susceptibility is almost constant [16]. However, periodicity of such a nonlinear grating enables one to phase match waves within a very narrow frequency band; the spectral interval of effective QPM becomes narrower when the crystal length is increased. This causes difficulties in the conversion of broadband cw or ultrashort pulsed radiation, conversion of images, cascaded conversion processes. Recently it was proposed to solve the problem for cascaded processes by using different orders of QPM [17,18], or special quasiperiodic domain gratings, such as Fibonacci-like or Cantor-like fractal structures [19–21]. Potentially, two-dimensional domain gratings in hexagonally poled crystals [22,23] can be also advantageous from this point of view. In any case, to control the frequency band of conversion processes, an additional (in comparison with periodic structures) degree of freedom is necessary. From a general viewpoint, disordering of optical QPM structures gives a possibility to obtain this degree. Several special types of disordered structures have already been studied previously, such as linearly chirped domain gratings for the frequency doubling of chirped femtosecond pulses [24,25], reset-periodic structures [26] and totally disordered domain gratings [27–29] for parametric generation, amplification and frequency conversion.

In all previous works, using of aperiodicity promises to be advantageous, but nonlinear interactions are considered separately for each new type of the disordered structure. At the same time, there should be quite general features in the behavior of all disordered nonlinear-optical structures in different parametric processes at their initial low-gain stages, when the nondepleted pump approximation is valid. If these features were clearly recognized, the problem of primary characterization of any disordered structure and its potentialities would be made substantially easier, and there would be a key to the engineering of an optimal nonlinear medium for a given application. The main goal of this work was to solve this problem for one-dimensional nonlinear-optical QPM structures with arbitrary nonperiodic variation of the second-order optical response. It was done by considering wave equations for three-wave parametric interactions in continuous (Sec. II) and pulsed (Sec. III) pumping regimes. As a result, it was shown that, in all the diversity of nonlinear processes considered, the impact of nonlinear medium spatial structure can be described in terms of a single functional parameter. This is a nonlinear transfer function (the "*T*-function"), which depicts the spatial distribution of the second-order susceptibility in a specific mode. Expressed in terms of dimensionless phase mismatches, it can be measured once in some process convenient for measuring, and further applied in another process, provided that the refractive indexes and dispersion of the medium are known. For its characterization we propose a method based on spontaneous parametric down-conversion (SPDC) [30]. The universal nature of the *T*-function and the SPDC method for its measurement are discussed in Sec. IV. Information on the *T*-function may be important in various problems, such as engineering the spectral shapes of terahertz-range signals, emitted via non-linear optical processes, the optimal detection of specially shaped signals, generation of squeezed light [31] or mode-structured quantum entangled states [32,33], and so on. Examples of possible applications of the *T*-function approach are considered in Sec. V. Finally, in Sec. VI, the conclusions are presented.

II. THREE-WAVE PARAMETRIC INTERACTION

Consider parametric interaction between two plane waves of frequencies ω_1 and ω_2 in a nonlinear medium with the spatial modulation of second-order susceptibility along one direction, $\chi^{(2)}(x)$. The interaction results in the generation of the third waves $E(\omega,x)e^{-i\omega t}$, of difference frequency $\omega=\omega_1-\omega_2$, or sum frequency $\omega=\omega_1+\omega_2$, according to the general wave equation:

$$\frac{\partial^2 E(\omega,x)}{\partial x^2}+\varepsilon(\omega)\frac{\omega^2}{c^2}E(\omega,x)=-\frac{4\pi\omega^2}{c^2}P^{(nl)}(\omega,x), \quad (1)$$

where $\varepsilon(\omega)$ is the dielectric function of the medium, $P^{(nl)}(\omega,x)$ is the nonlinear polarization, equal to $P^{(nl)}(\omega,x)=\chi^{(2)}(x)E_1(\omega_1,x)[E_2(\omega_2,x)]^*$ in the case of difference frequency generation or to $P^{(nl)}(\omega,x)=\chi^{(2)}(x)E_1(\omega_1,x)\times E_2(\omega_2,x)$ in the case of sum frequency generation.

An arbitrary spatial variation of the second-order susceptibility $\chi^{(2)}(x)$ within the medium length L along the x direction can be written as a Fourier series,

$$\chi^{(2)}(x)=\sum_{m=-\infty}^{\infty}\chi_m e^{im(2\pi/L)x}, \quad (2)$$

where χ_m are the amplitudes of spatial Fourier harmonics,

$$\chi_m=\frac{1}{\mathrm{L}}\int_{-L/2}^{L/2}\chi^{(2)}(x)e^{-im(2\pi/L)x}dx, \quad (3)$$

and $\chi_m=\chi_{-m}^*$.

In general, solution of the wave equation (1) yields two different waves, $E(\omega,x)=A_f(\omega,x)\exp(ik_x x-i\omega t)+A_b(\omega,x)\exp(-ik_x x-i\omega t)$, with the opposite projections k_x of the wave vectors $k=k(\omega)$ on the X axis. The amplitudes of forward $A_f(\omega,x)$ and backward $A_b(\omega,x)$ propagating waves are calculated as [34]

$$A_f(\omega,x)=\frac{2\pi i\omega^2}{kc^2}\int_{-L/2}^{x}P^{(nl)}(\omega,x')e^{-ik_x x'}dx', \quad (4a)$$

$$A_b(\omega,x)=\frac{2\pi i\omega^2}{kc^2}\int_{x}^{L/2}P^{(nl)}(\omega,x')e^{ik_x x'}dx'. \quad (4b)$$

Explicit expressions for the amplitudes $A_f(\omega,x)$ and $A_b(\omega,x)$ can be easily obtained in the low-gain approximation, where the incoming waves at frequencies ω_1 and ω_2 have almost constant amplitudes $A_1(\omega_1)$ and $A_2(\omega_2)$ within the whole medium length. Nevertheless, there can be considerable absorption at signal frequencies. In this case, k is complex, $k_x=k_x'+ik_x''$, and the reduced amplitudes $\bar{A}_f(\omega,L/2)\equiv A(\omega,L/2)e^{-k''L/2}$ and $\bar{A}_b(\omega,-L/2)\equiv A_b(\omega,-L/2)e^{k''L/2}$ describe the output signals generated in the two opposite directions. With an account for the expression (2) for $\chi^{(2)}(x)$, solutions for the reduced amplitudes take the forms

$$\bar{A}_f(\omega,L/2)=\frac{i2\pi\omega^2 L}{kc^2}e^{-\alpha L/4}T_f(\omega)C(\omega_1,\omega_2), \quad (5a)$$

$$\bar{A}_b(\omega,-L/2)=\frac{i2\pi\omega^2 L}{kc^2}e^{-\alpha L/4}T_b(\omega)C(\omega_1,\omega_2). \quad (5b)$$

Here, $C(\omega_1,\omega_2)$ are determined by the pump amplitudes, $C(\omega_1,\omega_2)=A_1(\omega_1)[A_2(\omega_2)]^*$ for difference-frequency generation and $C(\omega_1,\omega_2)=A_1(\omega_1)A_2(\omega_2)$ for sum-frequency generation, and $\alpha\equiv 2k_x''$ is equal to the absorption coefficient at the signal frequency ω for collinear interaction. The functions $T_f(\omega)$ and $T_b(\omega)$ describe the inhomogeneous distribution of the nonlinear susceptibility:

$$T_f(\omega)\equiv\sum_{m=-\infty}^{\infty}\chi_m f(\Delta_f+2\pi m), \quad (6a)$$

$$T_b(\omega)\equiv\sum_{m=-\infty}^{\infty}\chi_m f(\Delta_b+2\pi m). \quad (6b)$$

Here, Δ_f and Δ_b are dimensionless phase mismatches (DPM) for the forward and backward generation processes, correspondingly,

$$\Delta_f\equiv(k_{1x}\pm k_{2x}-k_x)L, \quad (7a)$$

$$\Delta_b\equiv-(k_{1x}\pm k_{2x}+k_x)L. \quad (7b)$$

$k_x, k_{jx}(j=1,2)$ are the x projections of the wave vectors, "+" stands for sum, and "−" for difference frequency generation. The form-factor $f(\delta)$ for any complex δ is determined as $f(\delta)\equiv(1/L)\int_{-L/2}^{L/2}e^{ix\delta/L}dx$; in a nonabsorptive medium it is reduced to $f(\delta)=\mathrm{sinc}(\delta/2)$.

As one can see from Eqs. (6), the functions $T_f(\omega)$ and $T_b(\omega)$, both for the sum- and difference-frequency processes, depend on the signal frequency ω via the same functional dependency on DPM. Various dependencies on the frequency ω are due to the differences in the DPM dispersion. Thus, as it follows from Eqs. (5) and (6), in all low-gain three-wave parametric interactions the influence of the spatial inhomogeneity of the nonlinear coefficient manifests itself in a very similar way: via the same transfer function, the "T-function,"

$$T(\Delta)\equiv\sum_{m=-\infty}^{\infty}\chi_m f(\Delta+2\pi m). \quad (8)$$

In the absence of absorption, the T-function turns into

$$T_0(\Delta)\equiv\sum_{m=-\infty}^{\infty}\chi_m\,\mathrm{sinc}\left(\frac{\Delta}{2}+\pi m\right). \quad (8a)$$

Expression (8) for the T-function in terms of DPM has a universal form and does not depend on the type of the three-wave process.

III. SUM- AND DIFFERENCE-FREQUENCY GENERATION UNDER SHORT-PULSE PUMPING

In a lot of applications, instead of monochromatic one- or two-wave pumping, a nonlinear medium is simply pumped by a single laser source of short (femtosecond-range) pulsed radiation. In particular, it takes place under frequency dou-

bling of this radiation [24,25], generation of terahertz-range (THz) waves via optical rectification [7–10], and THz waves detection by optical sampling [35–37]. Irradiation of a nonlinear medium by short laser pulses can be considered as pumping by a continuum of pairs of waves with various frequencies ω_1 and ω_2, belonging to the spectrum of the pulse. The wave equation (1), as well as relationships for its solution (4), remains valid for each spectral component of the generated wave. The only point that should be modified is the expression for the nonlinear polarization. It takes the integral form,

$$P^{(\mathrm{nl})}(\omega,x) = \frac{\chi^{(2)}(x)}{2\pi}\int_{-\infty}^{\infty}[E_p(x,t)]^2 e^{i\omega t}dt = \chi^{(2)}(x) \times \int_{-\infty}^{\infty} E_p(x,\omega_1)E_p(x,\omega-\omega_1)d\omega_1, \tag{9}$$

for sum-frequency generation, and

$$P^{(\mathrm{nl})}(\omega,x) = \frac{\chi^{(2)}(x)}{2\pi}\int_{-\infty}^{\infty}|E_p(x,t)|^2 e^{i\omega t}dt = \chi^{(2)}(x) \times \int_{-\infty}^{\infty} E_p(x,\omega_1)E_p^*(x,\omega_1-\omega)d\omega_1 \tag{10}$$

for difference frequency generation. Here, $E_p(x,t)$ is the time-dependent electric field of the pumping pulse and $E_p(x,\omega_1)$ is its temporal Fourier transform: $E_p(x,t) = \int_{-\infty}^{\infty} E_p(x,\omega_1)e^{-i\omega_1 t}d\omega_1$.

Analogues of expressions (5) for the amplitudes of the spectral components for the generated signals can be easily obtained when the group velocity dispersion is negligible within the spectral widths of the pump and signal pulses. In this approximation, under a sum-frequency process, dimensionless phase mismatches $\Delta_{f,b} \equiv \pm[k(\omega_0+\Omega_1)+k(\omega_0+\Omega_2) \mp k(2\omega_0+\Omega_2+\Omega_1)]L$ between each two spectral components of the pump (at the frequencies $\omega_0+\Omega_1$ and $\omega_0+\Omega_2$, detuned from the central pulse frequency ω_0) and one spectral component of the signal (at the frequency $\omega=2\omega_0+\Omega$, detuned from $2\omega_0$ by $\Omega=\Omega_1+\Omega_2$), are equal to

$$\Delta_f = \{2k(\omega_0) - k(2\omega_0) + (\omega-2\omega_0)[u^{-1}(\omega_0) - u^{-1}(2\omega_0)]\}L, \tag{11a}$$

$$\Delta_b = -\{2k(\omega_0) + k(2\omega_0) + (\omega-2\omega_0)[u^{-1}(\omega_0) + u^{-1}(2\omega_0)]\}L. \tag{11b}$$

Here, $u^{-1}(\omega_0)$ and $u^{-1}(2\omega_0)$ are inverse group velocities of the medium at the central frequencies of the pump (ω_0) and its second harmonic ($2\omega_0$). In the same way, DPMs for a difference-frequency process, $\Delta_{f,b} \equiv \pm[k(\omega_0+\Omega_1)-k(\omega_0+\Omega_2) \mp k(\Omega_1-\Omega_2)]L$, take forms

$$\Delta_f = \{\omega u^{-1}(\omega_0) - k(\omega)\}L, \tag{12a}$$

$$\Delta_b = -\{\omega u^{-1}(\omega_0) + k(\omega)\}L, \tag{12b}$$

describing the mismatches between each two spectral components of the pump (at the frequencies $\omega_0+\Omega_1$ and $\omega_0+\Omega_2$) and one spectral component of the signal (at the frequency $\omega=\Omega_1-\Omega_2$).

Within these approximations, the amplitudes $A_f(\omega,L/2)$ and $A_b(\omega,-L/2)$ of the forward and backward waves are very similar to Eq. (5),

$$\bar{A}_{f,b}(\omega,\pm L/2) = \frac{i2\pi\omega^2 L}{kc^2}e^{-\alpha L/4}T_{f,b}(\omega)C(\omega). \tag{13}$$

The only difference is in the C factor, which takes into account the pump amplitude distribution. For a sum-frequency process, this factor depends on the Fourier transform of the square of the time-domain envelope $B_p(t)$ of the pump field $E_p(x,t) \equiv B_p(t)e^{-i\omega_0 t+ik(\omega_0)x}$:

$$C(\omega) = C_{\mathrm{sum}}(\omega) \equiv \int_{-\infty}^{\infty} A_p(x,\Omega')A_p(x,\omega-2\omega_0-\Omega')d\Omega' = \frac{1}{2\pi}\int_{-\infty}^{\infty} B_p^2(t)e^{i(\omega-2\omega_0)t}dt. \tag{14a}$$

For a difference-frequency process, it depends on the Fourier transform of the pump pulse intensity:

$$C(\omega) = C_{\mathrm{dif}}(\omega) \equiv \int_{-\infty}^{\infty} A_p(x,\Omega')A_p^*(x,\Omega'-\omega)d\Omega' = \frac{1}{2\pi}\int_{-\infty}^{\infty}|B_p(t)|^2 e^{i\omega t}dt. \tag{14b}$$

The transfer functions $T_{f,b}(\omega) \equiv T(\Delta_{f,b})$ appear in Eq. (13) in the same form as in the case of an ordinary three-wave process. Thus, under short-pulse pumping, the influence of the spatial variation of the material nonlinear coefficient is also described by these functions, and again, only by them.

IV. *T*-FUNCTION AND ITS MEASUREMENT

The final expressions (5) and (13), obtained in previous sections, describe the spectral distributions of the waves generated in a nonlinear medium. It is of main importance for this treatment that the contribution of the pump temporal spectrum (via the C-function) and the contribution of the spatial spectrum of the medium inhomogeneity (via the T-function) always appear separately. Since these contributions can be separated, it is possible to make an independent characterization of the medium inhomogeneity. The T-function dependence on DPM characterizes potential applications of any given nonlinear sample and determines the optimal structure of the pump spectrum for the engineering of signal spectra in various applications. The inverse task is also important, when the sample with a necessary T-function is designed for any spectrum transformation required in a non-linear parametric process.

In ferroelectric nonlinear crystals, accessible modulation amplitudes of the second-order susceptibility $\chi^{(2)}(x)$ are the highest due to reversals of the sign of $\chi^{(2)}$ at the domain boundaries [38]. There are various methods [39–43] for structured poling of these materials, providing periodic or any special nonperiodic $\chi^{(2)}(x)$ dependence inside the

sample. In a periodically poled crystal, all harmonics χ_m are equal to zero except those whose numbers m_0 satisfy $m_0/(L/d)=m'$, where m' is integer and d is the structure period. The shape of the $\chi^{(2)}(x)$ distribution within the period determines the spectrum of χ_{m_0} [38,44,45]. Usually it is stepwise and there is no freedom for broad T-function engineering in periodically poled structures. The only possibilities are changing the period or the duty cycle, which leads to optimal quasiphase matching in a given nonlinear process, or, in terms of current treatment, helps to match the maxima of C- and T-functions. The situation is different in nonperiodically poled structures. Selecting necessary sequences of positive and negative domain thicknesses within the sample, one can affect the χ_m spectrum and build structures with different profiles of T-functions. It is possible, first of all, under postgrowth poling techniques. As-grown periodically poled crystals, obtained directly under the growth procedure [46,47], usually have sufficiently lower periodicity. After a proper characterization of their T-function they may also be selected for a specific application.

For any sample with a nonuniform distribution of $\chi^{(2)}$, the T-function can be measured by using various available nonlinear processes. Nevertheless, under stimulated parametric processes, as considered in the previous sections, the scale of accessible DPMs is limited by the pump spectrum. One needs to change the frequency of at least one pumping wave to change DPM sufficiently. According to Eqs. (7), it can be done by varying the pump angle of incidence, but this method is limited to a small range of DPM scanning and has a number of other disadvantages [44]. Among all possible low-gain three-wave parametric processes there is one that does not require tuning of the pump parameters: It is spontaneous parametric down-conversion (SPDC).

SPDC describes the initial under-threshold behavior of the output signal under optical parametric generation. It consists of the spontaneous decay of monochromatic pump photons (of frequency ω_1) into pairs of signal (frequency ω) and idler (frequency ω_2) photons, so that $\omega=\omega_1-\omega_2$. This process has a purely quantum origin [48] and is widely used now as a source of quantum correlated pairs of photons [49]. In many respects, it looks like a stimulated down-conversion process, or a difference-frequency generation, as if the role of the second (idler) pumping wave were played by zero vacuum fluctuations of the electromagnetic field [48,50]. But instead of the classical pump at the idler frequency ω_2 at the input of the medium, there is a continuum of quantum vacuum states of the electromagnetic field at all frequencies from 0 up to ω_1 everywhere inside the nonlinear medium, the generated signals occupy a broad spectral and angular range. Consistent treatment of frequency-angular distribution for the SPDC signals in periodically poled crystals was carried out previously [51], taking into account the quantum nature of the effect and possible absorption of the nonlinear medium. In particular, for the case where absorption at the idler frequency ω_2 is negligible, it was shown that the SPDC signal intensity distribution is the same as in the case of difference-frequency generation, when this stimulated process occurs under pumping by a continuum of idler modes of the same population: one photon per any idler mode at the input of the nonlinear sample.

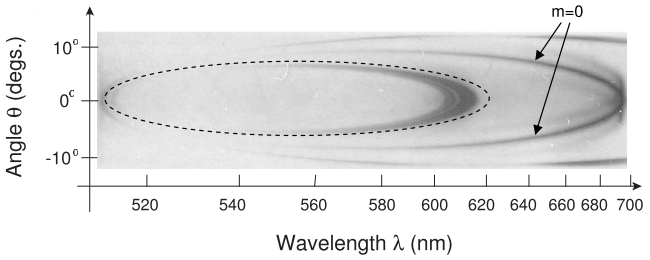

FIG. 1. A part of the photographic SPDC spectrum of $Y:LiNbO_3$ crystal with a nonregular domain grating. Arrows indicate the basic phase-matched tuning curve corresponding to $m=0$. The dashed line outlines the round area in which there are the quasi-phase-matched curves corresponding to the orders m between −500 and −700.

It is namely the case of negligible absorption that is important for measuring the universal T-function. In this case the measurement can be done in terms of real-value DPM in some spectral range, which is convenient for the registration of the SPDC spectra, and, after that, recalculated into another spectral range, in which the sample will operate. The information on the refractive index dispersion $n(\omega), n_1(\omega_1), n_2(\omega_1-\omega)$ should be known in both ranges. As to absorption coefficients (corresponding to the imaginary parts of DPM), they have to be taken into account only if the working parametric process takes place in the range of considerable absorption losses. Then absorption effects will lead to a homogeneous broadening of all line components of the basic ("lossless") T-function structure.

Generalizing the results of [51] for media with arbitrary spatial distributions $\chi^{(2)}(x)$, and using the T-function formalism, for the SPDC intensity in transparency ranges we obtain

$$I(\omega,\theta)=\frac{\hbar\omega^4(\omega_1-\omega)^2L^2}{nn_1k_{2x}c^6}I_1|T_0(\Delta_f)|^2. \tag{15}$$

Here, $I(\omega,\theta)$ is defined as the signal energy emitted at mean angle θ and frequency ω by a unit surface area into a unit solid angle per unit spectral interval per unit time, and I_1 stands for the pump intensity; the DPM Δ_f and its dependence on ω,θ are determined according to Eq. (7a) for difference frequency generation, taking ω_1, ω_2, and ω as the frequencies of the pump, idler, and signal waves, correspondingly. Thus, according to Eq. (15), one can tune the frequency ω and/or the angle of observation θ of the SPDC signal, and this way study the T-function distribution without changing the pump parameters. The experimental setup for the observation of frequency-angular SPDC spectra within large intervals of ω,θ was discussed previously (for example, see [30,38]).

Figures 1–3 present the result of such SPDC characterization of the basic T-function, made for a crystal of $Y:LiNbO_3$ with the as-grown domain structure. The primary study of the sample by selective chemical etching has shown that the domain thicknesses in the sample vary within 30–34 μm [47]. The SPDC spectrum in Fig. 1 was obtained under pumping by an ordinarily polarized Ar laser at a wavelength of 488 nm, directed along the X axis of the crystal, normally

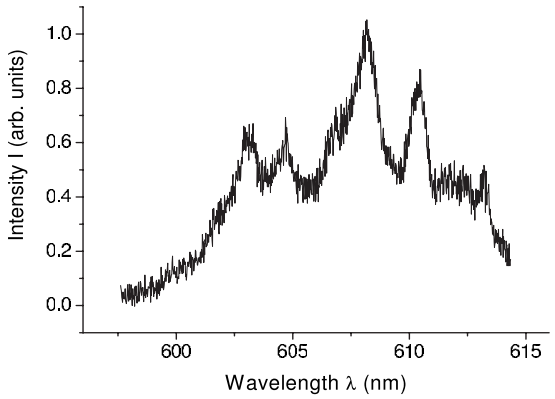

a.

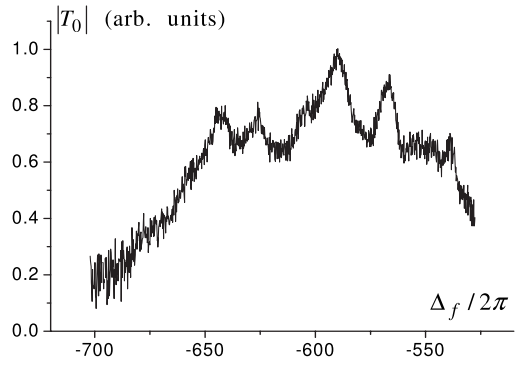

b.

FIG. 2. (a) Intensity of collinear quasi-phase-matched SPDC signal as a function of the signal wavelength [47]. (b) Distribution of the module of the crystal transfer function, calculated according to the SPDC data.

to domain layers. The spectrum was recorded by a photographic film at the output plane of a spectrograph [30]. The vertical angle sweep corresponds to the angle θ between the pump and signal waves emitted from the crystal. The horizontal spectral sweep is given in terms of signal wavelengths and represents the part of the whole spectrum in the transparency region. Since the data on the refractive index dispersion for this crystal is available [52–54], we can calculate the DPM Δ_f for each point in the plane ω, θ. We find that the narrow bright line corresponds to the zero-order quasiphase matching in the crystal, $m=0$. The group of low-intensity curves (outlined by a dashed line in Fig. 1) are attributed to quasiphase matching at higher orders of m, so as $-500 < m < -700$. It is necessary to recall that these values of m correspond to Fourier series expansion (2), which accounts for the whole crystal length instead of one period. In a perfect periodic structure with some constant period d, there should be only one tuning curve, numbered by the certain $m=m_0$. The corresponding value of $m' \equiv m_0/(L/d)$, which usually denotes the order of quasiphase matching in a periodic QPM structure, has to satisfy $m'=-1$. The appearance of a number of smoothed curves in this region of the spectrum directly indicates a nonperiodic character of the domain grating. Figure 2(a) shows the SPDC intensity distribution measured as a function of the signal wavelength at the zero angle θ for this group of quasi-phase-matched tuning curves. Precise intensity measurements were made by a Jobin Yvon T64000 spectrometer [47]. In principle, any intensity dependence of this type, measured by scanning the position of a small-area detector in the output plane of a spectrograph along any appropriate direction, parallel or inclined toward the spectrum axes, can be used as a starting point for subsequent characterization of the T-function. At the next step, the scale of signal frequencies is recalculated to the scale of DPM according to Eq. (7a). The scale of SPDC intensities is also recalculated into $|T_0(\Delta_f)|$ in relative units, taking into account other frequency-dependent factors in Eq. (15). Finally, Fig. 2(b) presents the result of SPDC characterization of the sample in terms of the T-function.It is made in the range of the most effectively quasiphase matched DPM. As it can be estimated from the photographic spectrum in Fig. 1, other areas of non-phase-matched interactions with $\Delta_f \neq 0$ correspond to much lower values of $|T_0(\Delta_f)|$.

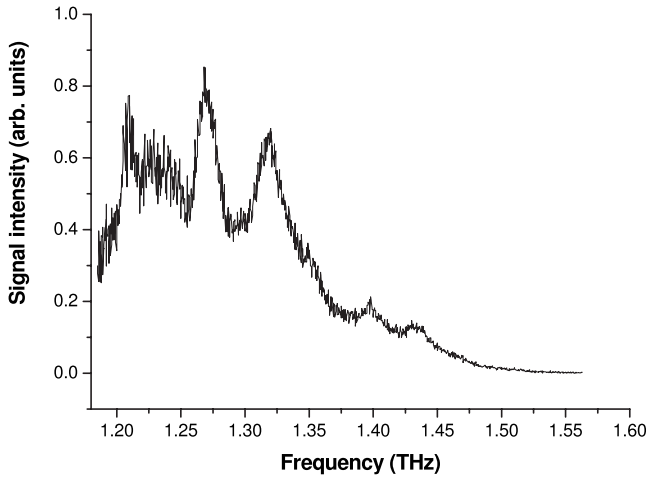

FIG. 3. Intensity of the backward generated THz signal as a function of THz frequency, calculated for a Y:$LiNbO_3$ crystal using SPDC data from Figs. 1 and 2.

V. APPLICATIONS OF T-FUNCTION ENGINEERING

A. Terahertz wave generation via optical rectification

Equation (13), taking into account Eq. (14b), describes directly the amplitudes of THz waves generated under optical rectification of a short-pulse pump at the input $(x=-L/2)$ and output $(x=+L/2)$ of a crystal sample,

$$\bar{A}_{\mathrm{THz},f}(\Omega, L/2) = \frac{i2\pi\Omega^2 L}{k_{\mathrm{THz}}c^2} e^{-\alpha_{\mathrm{THz}}L/4} T(\Delta_f) C_{\mathrm{dif}}(\Omega),$$

$$\bar{A}_{\mathrm{THz},b}(\Omega, -L/2) = \frac{i2\pi\Omega^2 L}{k_{\mathrm{THz}}c^2} e^{-\alpha_{\mathrm{THz}}L/4} T(\Delta_b) C_{\mathrm{dif}}(\Omega), \quad (16)$$

at a THz frequency $\Omega/2\pi$, where $k_{\mathrm{THz}}=k(\Omega)$. Usually, for periodically and quasiperiodically poled crystals and femtosecond pump pulses, the pump spectrum $C_{\mathrm{dif}}(\Omega)$ is much

wider than the spectrum of the crystal transfer function $T(\Delta_f)$ or $T(\Delta_b)$. In this case, the width of $C_{\mathrm{dif}}(\Omega)$ specifies only the maximal THz frequency, which is accessible using given pump pulse parameters. On the contrary, the peaks of the crystal functions $T(\Delta_{f,b})$ are considerably narrower in the THz frequency scale. They determine the width and details of spectra of both THz signals generated in forward and backward directions.

As an example, consider THz signals that can be generated in a $Y:LiNbO_3$ crystal with the T-function presented in Fig. 2(b). Substituting values of DPM from Fig. 2(b) into the basic relations (12a) and (12b), and taking into account dispersion parameters of undoped $LiNbO_3$ in THz [55,56] and optical [52–54] ranges, we calculate THz frequencies accessible for forward and backward generation in *eee* geometry. The forward generation gets into the range 2.8–3.2 THz, where the crystal absorption strongly reduces the THz output. At the same time, the backward signal corresponds to the range 1.2–1.5 THz, where absorption is rather small. Figure 3 presents the spectral distribution of backward THz signal intensity, estimated as $|\bar{A}_{\mathrm{THz},b}(\Omega,-L/2)|^2$, for the case of Gaussian pump pulses of 100 fs duration. The backward THz signal has a complex structure, following the structure of $|T_0(\Delta)|$, with an account for other frequency-dependent factors in Eq. (16). Thus, due to the universal character of the crystal transfer function, SPDC measurements in the visible frequency range enable one to predict the spectral shape of signals generated in the THz range.

It should be mentioned that such spectral transformations can be made directly if absorption is negligible, $\alpha L \ll 1$, for any absorption coefficients α at optical or THz frequencies involved into the processes. Otherwise, Δ becomes imaginary, $\Delta=\Delta'+i\Delta''$, and $|T(\Delta)|$ is smoothed [in comparison with $|T_0(\Delta)| \equiv |T_0(\Delta')|$]. Due to the large spectrum of quasi-phase-matched SPDC, it is not difficult to find spectral intervals where absorption of the pump, signal and idler waves is negligible and to measure $|T_0(\Delta')|$. This information will be quite precise for predicting the spectral characteristics for applications in transparency ranges, but will be not able to describe the widths of "fine structure" maxima in the ranges of considerable absorption.

B. Terahertz wave detection via frequency mixing

Nonlinear parametric processes can be used not only for the energy transfer from optical to terahertz ranges, but also for the reverse energy transfer from the terahertz to optical range. This reverse transfer is useful for the detection of terahertz radiation by means of various sensitive methods, developed for visible and near-visible frequency ranges.

In the general scheme of terahertz detection via frequency conversion, mutually coherent terahertz and optical pulses, delayed from each other, are incident to a crystal. An optical registration system, placed after the crystal, measures the changes of the probe beam transmittance induced by the terahertz field, as a function of the time delay between terahertz and optical pulses. Properly oriented polarizer and analyzer may be placed before and after the crystal, respectively, to control the working point of the measurement. In well-known schemes of electro-optical sampling [35,36,57], this point may be made close to zero owing to a special selection of the type of nonlinear interaction, *ooe*: The polarizer and analyzer are crossed, and the transmitted optical radiation appears only due to the parametric interaction between optical and terahertz pulses. Fundamentally, this is not necessary, and *eee* types of nonlinear interaction in periodically (or aperiodically) poled crystals are also possible for the THz wave detection. The technical problem of measuring relatively small THz-induced changes of the probe beam transmittance against a strong background is solved by using a lock-in amplifier [10,37].

To calculate the spectral sensitivity of these terahertz detectors of up-conversion type, consider a nonlinear interaction between some spectral component $A_{\mathrm{THz}}(\Omega)\exp\{i[k_{\mathrm{THz}}(\Omega)x-\Omega t]\}$ of the input THz pulse and the whole spectrum $A_{\mathrm{pr}}(\omega,x)\exp\{i[k_{\mathrm{pr}}(\omega)x-\omega t]\}$ of the probe optical pulse inside the crystal. Variation of the probe amplitude $A_{\mathrm{pr}}(\omega,x)$ during its forward propagation along the X axis is determined according to Eq. (4a), where nonlinear polarization consists of two terms,

$$P^{(\mathrm{nl})}(\omega,x) = \chi(x)\{A_{\mathrm{pr}}(\omega-\Omega)A_{\mathrm{THz}}(\Omega)\exp[ik_{\mathrm{pr}}(\omega-\Omega)x + ik_{\mathrm{THz}}(\Omega)x] + A_{\mathrm{pr}}(\omega+\Omega)A^*_{\mathrm{THz}}(\Omega) \times \exp[ik_{\mathrm{pr}}(\omega+\Omega)x - ik_{\mathrm{THz}}(\Omega)x]\}. \quad (17)$$

The first term is due to a sum-frequency conversion process between a THz component at the frequency Ω and an optical component at the frequency $\omega-\Omega$, and the second one is due to a difference-frequency process between a THz component at the frequency Ω and an optical component at the frequency $\omega+\Omega$. To a high accuracy, the wave vectors $k_{\mathrm{pr}}(\omega+\Omega)$ and $k_{\mathrm{pr}}(\omega-\Omega)$ can be written as $k_{\mathrm{pr}}(\omega)+\Omega/u(\omega)$ and $k_{\mathrm{pr}}(\omega)-\Omega/u(\omega)$, respectively. Also, the probe amplitude $A_{\mathrm{pr}}(\omega,x)$ can be estimated as $A_{\mathrm{pr}}(\omega,x)=A_{\mathrm{pr}}(\omega)+\Delta A_{\mathrm{pr}}(\omega,\Omega,x)$, where the nonlinear term $\Delta A_{\mathrm{pr}}(\omega,\Omega,x)$, appearing due to the mixing with the THz wave of frequency Ω is much smaller than the constant part $A_{\mathrm{pr}}(\omega)$. Variation of the THz amplitude in the course of its propagation in the crystal can also be neglected in Eq. (17). Possible absorption of the THz wave is taken into account in the imaginary part of its wave vector. Within these realistic approximations, the expression for the amplitude change $\Delta A_{\mathrm{pr}}(\omega,\Omega,L/2)$ at the output of the crystal is obtained in terms of the T-function as

$$\Delta A_{\mathrm{pr}}(\omega,\Omega,L/2) = \frac{2\pi i\omega^2}{k_{\mathrm{pr}}c^2}L[A_{\mathrm{pr}}(\omega+\Omega)A^*_{\mathrm{THz}}(\Omega)T(\Delta^*_f) + A_{\mathrm{pr}}(\omega-\Omega)A_{\mathrm{THz}}(\Omega)T^*(\Delta^*_f)]. \quad (18)$$

The optical registration scheme measures the THz-induced additive to the probe pulse energy, $\Delta P_\Omega = \int dt[I(t,\tau_{\mathrm{del}})-I_0(t)]$, where $I(t,\tau_{\mathrm{del}})=|\int_{-\infty}^{\infty}d\omega[A_{\mathrm{pr}}(\omega)+\Delta A_{\mathrm{pr}}(\omega,\Omega,L/2)]e^{-i\omega t}|^2$ is proportional to the probe pulse intensity measured in the presence of the THz pulse and

$I_0(t)=\left|\int_{-\infty}^{\infty}d\omega\, A_{\mathrm{pr}}(\omega)e^{-i\omega t}\right|^2$ corresponds to the same intensity in its absence. Integration runs over the probe pulse duration; τ_{del} is the delay time of the probe pulse. Taking into account Eq. (18), the registration scheme readout should be related to the THz amplitude as

$$\Delta P_\Omega = c_0 L\Omega\ \mathrm{Im}[C_{\mathrm{dif}}(\Omega)A^*_{\mathrm{THz}}(\Omega)T(\Delta_f)e^{i\Omega\tau_{\mathrm{del}}}], \qquad (19)$$

where c_0 is a constant, $C_{\mathrm{dif}}(\Omega)$ is the Fourier transform of the undelayed probe-pulse intensity [see Eq. (14b)]. Generally, the THz amplitude, the crystal transfer function, and the probe pulse Fourier transform have complex values: $A_{\mathrm{THz}}=|A_{\mathrm{THz}}|e^{i\varphi_{\mathrm{THz}}}$, $T(\Delta_f)\equiv|T(\Omega)|e^{i\varphi_T(\Omega)}$, and $C_{\mathrm{dif}}(\Omega)=|C(\Omega)|e^{i\varphi_{\mathrm{prob}}(\Omega)}$. In terms of their absolute values and phases, the registration scheme readout is

$$\Delta P_\Omega(\tau_{\mathrm{del}}) = c_0 L\Omega|T(\Delta_f)|\times|C(\Omega)|\times|A_{\mathrm{THz}}|\sin[\Omega\tau_{\mathrm{del}}-\varphi_{\mathrm{THz}}+\varphi_0(\Omega)], \qquad (19a)$$

where $\varphi_0(\Omega)\equiv\varphi_T(\Omega)+\varphi_{\mathrm{prob}}(\Omega)$. As it follows from Eq. (19a), the variation of ΔP_Ω under the time delay change has a sinusoidal character with the THz-wave period. Since the amplitude of this variation is linearly dependent on the absolute value of the THz amplitude, $|A_{\mathrm{THz}}|$ can be determined by analyzing the $\Delta P_\Omega(\tau_{\mathrm{del}})$ dependence. The product $S(\Omega)\equiv\Omega|C(\Omega)|L|T(\Delta_f)|$ comes out as a spectral sensitivity function for the whole THz-measurement device. Normally, a THz pulse consists of a lot of spectral components at different THz frequencies Ω, $E_{\mathrm{THz}}(t,x)=\int A_{\mathrm{THz}}(\Omega)e^{-i\Omega t+ik_{\mathrm{THz}}x}d\Omega$, and the registration system measures the integral sum $\Delta P\sim\int\Delta P_\Omega e^{-i\Omega\tau_{\mathrm{del}}}d\Omega$. The sensitivity function $S(\Omega)$ obtained above describes the genuine relation between the spectral components of the THz pulse and the transmittance changes $\Delta P(\tau_{\mathrm{del}})$.

In bulk crystals, periodically poled ones, or any other crystals with a given regular variation of $\chi^{(2)}(x)$, the distribution of the T-function phases is known in advance. For example, in bulk crystals, $T(\Delta_f)=\chi_0\,\mathrm{sinc}(\Delta/2)$, and $\varphi_T(\Omega)=0$. In these cases one can easily determine from Eq. (19a) not only the modules $|A_{\mathrm{THz}}|$, but also the phases of THz wave components, $\varphi_{\mathrm{THz}}(\Omega)$. For crystals with stochastic domain structures, the phase dependencies $\varphi_T(\Omega)$ can be very complicated, and the possibility of measuring for THz phases $\varphi_{\mathrm{THz}}(\Omega)$ remains under question. Nevertheless, the modules $|A_{\mathrm{THz}}|$ can be determined if the T-function module is measured via SPDC method. The use of crystals with stochastic domain structures provides a possibility of THz measurements in a wide spectral range. The spectral sensitivity of such detectors will be lower than in the case of bulk or periodically poled crystals, but they will operate in larger spectral intervals. In comparison with applications of non-phase-matched parametric processes in crystals with the same value of bulk nonlinear coefficients, which also can provide the increase of the spectral range for THz detection, this method is substantially more efficient.

Nonlinear interactions involved into pump-probe measurements of the THz response, used in [10] for the characterization of periodically poled crystals, can be regarded as cascaded processes, consisting of generation and internal detection of THz waves inside one and the same crystal. Made in terms of the T-function, subsequent treatment of these processes in a crystal with an arbitrary modulation $\chi^{(2)}(x)$ yields

$$\Delta P_\Omega = |C(\Omega)|^2\Omega^3L^2\left|\frac{1}{k_{\mathrm{THz}}}\left\{\sum_{m=-\infty}^{\infty}\chi_m\left[-\frac{T(-\Delta_f)\exp[(i\Delta_f/2)](-1)^m-\chi_m^*}{\Delta_f-2\pi m}-\frac{T(-\Delta_b)\exp[-(i\Delta_b/2)](-1)^m-\chi_m^*}{\Delta_b-2\pi m}\right]\right\}\right|. \qquad (20)$$

In case of negligible absorption, this expression takes the form

$$\Delta P_\Omega \approx |C(\Omega)|^2\Omega^3L^2\frac{|T(\Delta_f)|^2+|T(\Delta_b)|^2}{k_{\mathrm{THz}}}. \qquad (20a)$$

As an example, for one of the crystal samples studied previously in the pump-probe scheme [10], we have calculated the spectral components ΔP_Ω for the induced probe beam transmittance according to Eq. (20a), at that using the results of $|T(\Delta)|$ measurements by the SPDC method. As it is seen from Fig. 4, calculated and directly measured dependencies, taken in the range of a well-pronounced experimental peak of forward generation, are in a good agreement. SPDC measurements of the T-function together with the reliable data [52–56] on the crystal dispersion properties in the optical and THz ranges were able to predict the shape and position of the measured line with a high accuracy.

C. Pulse shaping under ultrashort-pulse second harmonic generation

In the general case, the frequency doubling of ultrashort-pulse laser radiation may lead to a modification of the pulse spectrum. According to the results of the previous sections, the spectral distribution of the second-harmonic (SH) amplitude is described as

$$A(\omega,L/2) = i(2\pi\omega^2L/kc^2)T(\Delta_f)C_{\mathrm{sum}}(\omega), \qquad (21)$$

being determined not only by the pump field spectrum $C_{\mathrm{sum}}(\omega)$, but also by the crystal T-function. This means that

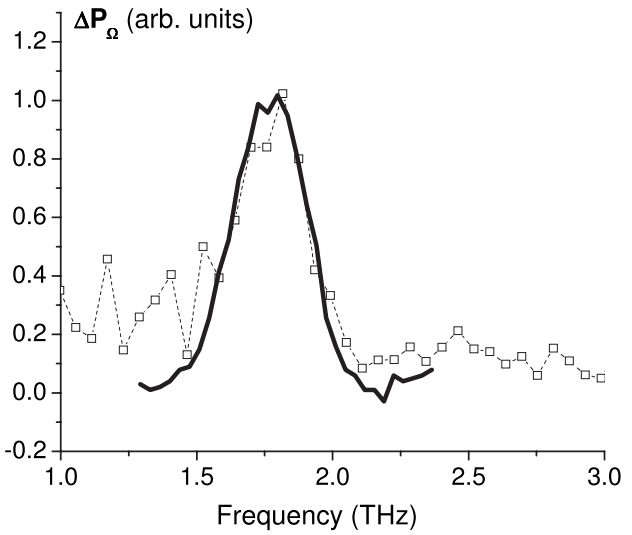

FIG. 4. Spectral components of the pump-probe signal as functions of THz frequency for a periodically poled $Mg:Y:LiNbO_3$ crystal, measured directly (dashed line [10]) and predicted according to SPDC data on the crystal transfer function (solid line).

by choosing a sample with a properly wide T-function, one can provide frequency conversion for all spectral components of the pump. It may be important for the frequency conversion of broadband continuous-wave radiation. Conversion of the whole frequency band can be simultaneously accessible under the same orientation of the nonlinear element. As for ultrashort-pulsed laser radiation, usually there is a necessity to keep a pulse duration no longer than that before frequency doubling. This also necessarily requires a sufficiently wide spectral distribution for the T-function.

As it follows from Eq. (21), the time-domain envelope of the SH field depends on the T-function of the crystal sample as

$$B_2(t) = 2\pi i \frac{L}{n_2 c} \int (\tilde{\Omega} + 2\omega_o) T(\Delta_f) C_{\text{sum}}(\tilde{\Omega}) \times e^{-i\tilde{\Omega}\{t-[u^{-1}(2\omega_o)]L/2\}} d\tilde{\Omega}, \quad (22)$$

where $\tilde{\Omega} = \omega - 2\omega_o$ is frequency detuning, and dependency of Δ_f on $\omega \equiv 2\omega_o + \tilde{\Omega}$ is given by Eq. (11a). To preserve the time duration of the SH pulse, or to make it even slightly shorter, bulk or ideal periodically poled crystals are used as a rule, but their length L has to be small enough—about hundreds of microns for femtosecond pulses [58]. Indeed, the shape of $T(\Delta_f)$ is given by $\chi_m \operatorname{sinc}[\Delta_f(\omega)/2 + \pi m]$, where $m=0$ in the case of a bulk crystal, or $m = \pm L/d$ in most cases of periodically poled crystals. The widths of bulk and quasi-phase-matched maxima are the same for regular structures, corresponding to the condition $|\Delta k| \leq 2\pi/L$. So, the simplest way to provide $T(\Delta_f) \neq 0$ in a broad spectral range is to make L small. However, this reduces the overall conversion efficiency. It may be more favorable to increase the width of $T(\Delta_f)$ by taking aperiodically poled crystals, in which $T(\Delta_f)$ consists of a large sequence of neighboring sinc-functions. As it is clear from Eq. (22), this possibility can be realized only when the overlap function $B_p(t)$ is complex. Then a narrow $|B_2(t)|$ can be obtained by a special choice of the phases of complex χ_m.

VI. CONCLUSIONS

We have studied the influence of nonregular spatial distribution of the second-order susceptibility on the spectral characteristics of nonlinear optical signals generated in inhomogeneous structures. General expressions were obtained for the amplitudes of the waves emitted in sum- and difference-frequency parametric processes both in forward and backward directions, under continuous and short-pulse pumping regimes.

It is shown that in the simplest approximation of constant pump and linear amplification, the spatial inhomogeneity of nonlinear properties determines the spectral shape of the generated signals via the crystal transfer function, the *T-function*. Expressed in terms of dimensionless phase mismatches Δ, this function $T(\Delta)$ has a universal character and appears in various optical parametric processes. The type of the process determines only the dependence of Δ on the frequencies involved. A method for the prior measurement of $T(\Delta)$ is proposed, based on spontaneous parametric down-conversion in the visible range. The results of such characterization of crystals with stochastic domain structures, designed for applications in terahertz range, are presented.

Various profiles of the T-function can be designed in ferroelectric multiply domained crystals. In periodically poled crystals, T-functions consist of series of isolated maxima, the shape of each line repeating the shape of the T-function of a bulk uniform crystal. In aperiodically poled crystals, special design of the T-function shape is possible. This opens a valuable possibility to control the spectral shape of quasi-phase-matched parametric signals. Frequency conversion processes can proceed with equal efficiency in large spectral and angular ranges simultaneously, for the same orientation of the nonlinear element. Different applications of this effect, possible under short-pulse pumping, are considered: designing the spectral shapes of generated and detected THz signals, as well as pulse shaping under second harmonic generation.

ACKNOWLEDGMENTS

This work is supported by the Program of supporting the leading scientific groups of Russia (Grant No. 4586.2006.2) and by grants of Russian Foundation for Basic Research Nos. 05-02-16278, 05-02-16391, and 07-02-91581.

[1] J. Armstrong, N. Bloembergen, J. Ducuing, and P. S. Pershan, Phys. Rev. **127**, 1918 (1962).
[2] P. A. Franken and J. F. Ward, Rev. Mod. Phys. **35**, 23 (1963).
[3] Y. H. Xue, N. B. Ming, J. S. Zhu, and D. Feng, Chin. J. Phys. (Taipei) **4**, 554 (1984).
[4] A. Feisst and P. Koidl, Appl. Phys. Lett. **47**, 1125 (1985).
[5] A. L. Aleksandrovskiĭ, G. Kh. Kitaeva, S. P. Kulik, and A. N. Penin, Sov. Phys. JETP **63**, 613 (1986).
[6] R. L. Byer, J. Nonlinear Opt. Phys. Mater. **6**, 549 (1997).
[7] Y.-S. Lee, T. Meade, M. DeCamp, and T. B. Norris, Appl. Phys. Lett. **77**, 1244 (2000).
[8] C. Weiss, G. Torosyan, J.-P. Meyn, R. Wallenstein, and R. Beigang, Opt. Express **8**, 497 (2001).
[9] J. A. L'Huillier, G. Torosyan, M. Theuer, Y. Avetisyan, and R. Beigang, Appl. Phys. B: Lasers Opt. **86**, 185 (2007).
[10] G. H. Ma, G. Kh. Kitaeva, I. I. Naumova, and S. H. Tang, J. Opt. Soc. Am. B **23**, 81 (2006).
[11] K. Mizuuchi, A. Morikawa, T. Sugita, and K. Yamamoto, Opt. Lett. **28**, 935 (2003).
[12] K. Moutzouris, F. Sotier, F. Adler, and A. Leitenstorfer, Opt. Express **14**, 1905 (2006).
[13] J. W. Haus, R. Viswanathan, M. Scalora, A. G. Kalocsai, J. D. Cole, and J. Theimer, Phys. Rev. A **57**, 2120 (1998).
[14] M. Scalora, M. J. Bloemer, A. S. Manka, J. P. Dowling, C. M. Bowden, R. Viswanathan, and J. W. Haus, Phys. Rev. A **56**, 3166 (1997).
[15] M. M. Fejer, G. A. Magel, D. H. Jundt, and R. L. Byer, IEEE J. Quantum Electron. **28**, 2631 (1992).
[16] A. L. Aleksandrovskiĭ, O. A. Gliko, I. I. Naumova, and V. I. Pryalkin, Quantum Electron. **26**, 641 (1996).
[17] A. S. Chirkin, J. Opt. B: Quantum Semiclassical Opt. **4**, S1 (2002).
[18] A. S. Chirkin, V. V. Volkov, G. D. Laptev, and E. Yu. Morozov, Quantum Electron. **30**, 847 (2000).
[19] S. N. Zhu, Y. Y. Zhu, and N. B. Ming, Science **278**, 843 (1997).
[20] X. Liu, Z. Wang, J. Wu, and N. Ming, Phys. Rev. A **58**, 4956 (1998).
[21] C. Sibilia, F. Tropea, and M. Bertolotti, J. Mod. Opt. **45**, 2255 (1998).
[22] N. G. R. Broderick, G. W. Ross, H. L. Offerhaus, D. J. Richardson, and D. C. Hanna, Phys. Rev. Lett. **84**, 4345 (2000).
[23] P. Xu, S. H. Ji, S. N. Zhu, X. Q. Yu, J. Sun, H. T. Wang, J. L. He, Y. Y. Zhu, and N. B. Ming, Phys. Rev. Lett. **93**, 133904 (2004).
[24] G. Imeshev, M. A. Arbore, M. Fejer, A. Galvanauskas, M. Fermann, and D. Harter, J. Opt. Soc. Am. B **17**, 304 (2000).
[25] P. Loza-Alvarez, M. Ebrahimzadeh, V. Sibbett, D. T. Reid, D. Artigas, and M. Missey, J. Opt. Soc. Am. B **18**, 1212 (2001).
[26] H. Guo, S. H. Tang, Y. Qin, and Y. Y. Zhu, Phys. Rev. E **71**, 066615 (2005).
[27] M. Baudrier-Raybaut, R. Haidar, Ph. Kupecek, Ph. Lamasson, and E. Rosencher, Nature (London) **432**, 374 (2004).
[28] X. Vidal and J. Martorell, Phys. Rev. Lett. **97**, 013902 (2006).
[29] E. Yu. Morozov, A. A. Kaminskii, A. S. Chirkin, and D. B. Yusupov, JETP Lett. **73**, 1090 (2006).
[30] G. Kh. Kitaeva and A. N. Penin, JETP Lett. **82**, 388 (2005).
[31] K. S. Zhang, T. Coudreau, M. Martinelli, A. Maitre, and C. Fabre, Phys. Rev. A **64**, 033815 (2001).
[32] A. V. Burlakov, M. V. Chekhova, O. A. Karabutova, and S. P. Kulik, Phys. Rev. A **63**, 053801 (2001).
[33] S. Carrasco, J. P. Torres, L. Torner, A. Sergienko, B. E. A. Saleh, and M. C. Teich, Phys. Rev. A **70**, 043817 (2004).
[34] Y. R. Shen, *The Principles of Nonlinear Optics* (John Wiley &Sons, New York, 1984), Chap. 8, pp. 110-116.
[35] A. Nahata, A. S. Weling, and T. F. Heinz, Appl. Phys. Lett. **69**, 2321 (1996).
[36] J.-P. Caumes, L. Videau, C. Rouyer, and E. Freysz, Phys. Rev. Lett. **89**, 047401 (2002).
[37] G. H. Ma, G. Kh. Kitaeva, I. I. Naumova, and S. H. Tang, Ferroelectrics **341**, 125 (2006).
[38] G. Kh. Kitaeva and A. N. Penin, Quantum Electron. **34**, 597 (2004).
[39] A. V. Golenishev-Kutuzov, V. A. Golenishev-Kutuzov, and R. I. Kalimullin, Phys. Usp. **43**, 663 (2000).
[40] L. E. Myers, R. C. Eckardt, M. M. Fejer, R. L. Byer, W. R. Bosenberg, and J. W. Pierce, J. Opt. Soc. Am. B **12**, 2102 (1995).
[41] S. N. Zhu, Y. Y. Zhu, and Z. Y. Zhang, J. Appl. Phys. **77**, 5481 (1995).
[42] H. Ito, C. Takyu, and H. Inaba, Electron. Lett. **27**, 1221 (1991).
[43] J. He, S. H. Tang, Y. Q. Qin, P. Dong, H. Z. Zhang, C. H. Kang, W. X. Sun, and Z. X. Shen, J. Appl. Phys. **93**, 9943 (2003).
[44] G. Kh. Kitaeva, V. V. Tishkova, and A. N. Penin, J. Raman Spectrosc. **36**, 116 (2005).
[45] K. A. Kuznetsov, H. C. Guo, G. KH. Kitaeva, A. A. Ezhov, D. A. Muzychenko, A. N. Penin, and S. H. Tang, Appl. Phys. B: Lasers Opt. **83**, 273 (2006).
[46] I. I. Naumova, N. F. Evlanova, O. A. Gliko, and S. V. Lavrishchev, J. Cryst. Growth **180**, 160 (1997).
[47] G. Kh. Kitaeva, V. V. Tishkova, I. I. Naumova, A. N. Penin, C. H. Kang, and S. H. Tang, Appl. Phys. B: Lasers Opt. **81**, 645 (2005).
[48] D. N. Klyshko, *Photons and Nonlinear Optics* (Gordon & Breach, NewYork, 1988).
[49] A. V. Burlakov, M. V. Chekhova, D. N. Klyshko, S. P. Kulik, A. N. Penin, Y. H. Shih, and D. V. Strekalov, Phys. Rev. A **56**, 3214 (1997).
[50] G. Kh. Kitaeva, A. N. Penin, V. V. Fadeev, and Yu. A. Yanait, Sov. Phys. Dokl. **24**, 564 (1979).
[51] G. Kh. Kitaeva and A. N. Penin, JETP **98**, 272 (2004).
[52] D. E. Zelmon, D. L. Small, and D. Jundt, J. Opt. Soc. Am. B **14**, 3319 (1997).
[53] G. Kh. Kitaeva, I. I. Naumova, A. A. Mikhailovsky, P. S. Losevsky, and A. N. Penin, Appl. Phys. B: Lasers Opt. **66**, 201 (1998).
[54] G. Kh. Kitaeva, K. A. Kuznetsov, A. N. Penin, and A. V. Shepelev, Phys. Rev. B **65**, 054304 (2002).
[55] U. T. Schwarz and M. Maier, Phys. Rev. B **53**, 5074 (1996).
[56] T. Qiu and M. Maier, Phys. Rev. B **56**, R5717 (1997).
[57] D. H. Auston and M. C. Nuss, IEEE J. Quantum Electron. **24**, 184 (1988).
[58] M. A. Arbore, M. Fejer, M. Fermann, A. Hariharan, A. Galvanauskas, and D. Harter, Opt. Lett. **22**, 13 (1997).